YEARLY TECHNICAL PROGRESS REPORT

submitted to

U. S. Department of Energy

Reporting Periods: 09/2704 – 09/26/05

December 26, 2005

Title: **Intelligent Monitoring System With High Temperature Distributed Fiberoptic Sensor For Power Plant Combustion Processes**

Authors: **Kwang Y. Lee, Stuart S. Yin, Andre Boheman**

The Pennsylvania State University
Department of Electrical Engineering
University Park, PA 16802
Ph. (814) 865-2621, Fax (814) 865-7065
kwanglee@psu.edu

Grant Number: DE-FG26-02NT41532
Performance Period: 09/27/2002 to 09/26/2005

DISCLAIMER

ABSTRACT

The objective of the proposed work is to develop an intelligent distributed fiber optical sensor system for real-time monitoring of high temperature in a boiler furnace in power plants. Of particular interest is the estimation of spatial and temporal distributions of high temperatures within a boiler furnace, which will be essential in assessing and controlling the mechanisms that form and remove pollutants at the source, such as NOx. The basic approach in developing the proposed sensor system is three fold: (1) development of high temperature distributed fiber optical sensor capable of measuring temperatures greater than 2000 C degree with spatial resolution of less than 1 cm; (2) development of distributed parameter system (DPS) models to map the three-dimensional (3D) temperature distribution for the furnace; and (3) development of an intelligent monitoring system for real-time monitoring of the 3D boiler temperature distribution.

Under Task 1, we set up a dedicated high power, ultrafast laser system for fabricating in-fiber gratings in harsh environment optical fibers, successfully fabricated gratings in single crystal sapphire fibers by the high power laser system, and developed highly sensitive long period gratings (lpg) by electric arc. Under Task 2, relevant mathematical modeling studies of NOx formation in practical combustors. Studies show that in boiler systems with no swirl, the distributed temperature sensor may provide information sufficient to predict trends of NOx at the boiler exit. Under Task 3, we investigate a mathematical approach to extrapolation of the temperature distribution within a power plant boiler facility, using a combination of a modified neural network architecture and semigroup theory. The 3D temperature data is furnished by the Penn State Energy Institute using FLUENT. Given a set of empirical data with no analytic expression, we first develop an analytic description and then extend that model along a single axis. Extrapolation capability was demonstrated for estimating enthalpy in a power plant.

TABLE OF CONTENTS

TECHNICAL PROGRESS REPORT

TABLE OF CONTENTS (Continued)

TECHNICAL PROGRESS REPORT

December 26, 2005

Title: **Intelligent Monitoring System With High Temperature Distributed Fiberoptic Sensor For Power Plant Combustion Processes**

Authors: Kwang Y. Lee, Stuart S. Yin, Andre Boheman
Students: J.A. Chavez, S.H. Nam, C. Zhan, Melanie Fox, B.H. Kim, John Valas
The Pennsylvania State University
Department of Electrical Engineering
University Park, PA 16802
Ph. (814) 865-2621, Fax (814) 865-7065
kwanglee@psu.edu
Grant Number: DE-FG26-02NT41532
Performance Period: 09/27/2002 to 09/26/2005

OVERVIEW AND PROGRESS TO DATE

The objective of the proposed work is to develop an intelligent distributed fiber optical sensor system for real-time monitoring of high temperature in a boiler furnace in power plants. Of particular interest is the estimation of spatial and temporal distributions of high temperatures within a boiler furnace, which will be essential in assessing and controlling the mechanisms that form and remove pollutants at the source, such as NOx.

The basic approach in developing the proposed sensor system is three fold: (1) development of high temperature distributed fiber optical sensor capable of measuring temperatures greater than 2000 C degree with spatial resolution of less than 1 cm; (2) development of distributed parameter system (DPS) models to map the three-dimensional (3D) temperature distribution for the furnace; and (3) development of an intelligent monitoring system for real-time monitoring of the 3D boiler temperature distribution.

Under Task 1, we set up a dedicated high power, ultrafast laser system for fabricating in-fiber gratings in harsh environment optical fibers, successfully fabricated gratings in single crystal sapphire fibers by the high power laser system, and developed highly sensitive long period gratings (lpg) by electric arc. Under Task 2, relevant mathematical modeling studies of NOx formation in practical combustors. Studies show that in boiler systems with no swirl, the distributed temperature sensor may provide information sufficient to predict trends of NOx at the boiler exit. Under Task 3, we investigate a mathematical approach to extrapolation of the temperature distribution within a power plant boiler facility, using a combination of a modified neural network architecture and semigroup theory. The 3D temperature data is furnished by the Penn State Energy Institute using FLUENT. Given a set of empirical data with no analytic expression, we first develop an analytic description and then extend that model along a single axis. Extrapolation capability was demonstrated for estimating enthalpy in a power plant.

TASK 1. FIBEROPTIC SENSOR DEVELOPMENT

1.1 Objectives and Motivations

The objective of this task is to develop an innovative high temperature distributed fiber optic sensor by fabricating in-fiber gratings in single crystal sapphire fibers. This unique high temperature distributed fiber optic sensor can precisely monitor the temperature distribution inside a boiler, which, in turn, could substantially increase the burning efficiency and reduce the pollution emission (e.g., NO_x). Figures 1 illustrates a boiler with embedded fiber optic sensors.

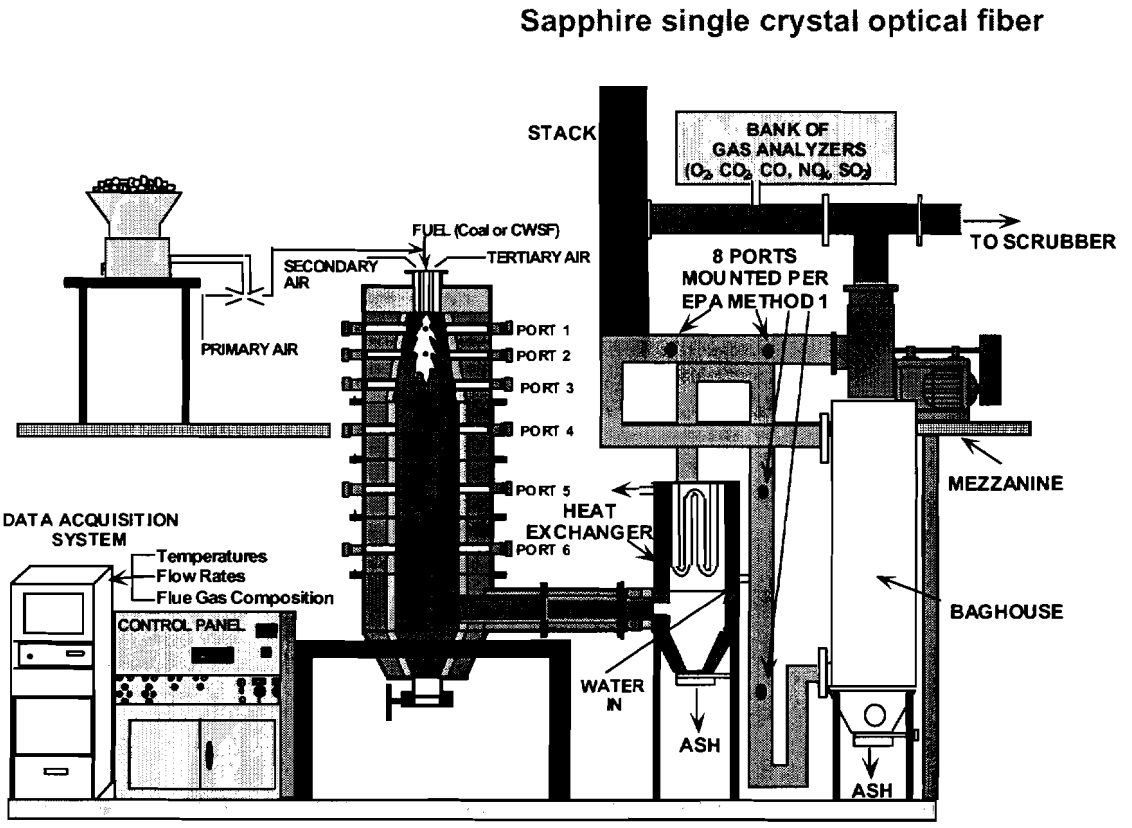

Fig. 1 (b) A boiler with embedded fiber optic sensor.

In the third year, we continuously improve the performance of high temperature distributed fiber optic sensor by using new configuration (such as radiation modal coupling) and new in-fiber grating fabrication approach (such as plasma etching), which can relax the quality requirement (e.g., transparency) on alumina cladding that in turn reduce the complexity for the sensor fabrication and increase practicability of the sensor.

To the best knowledge of authors, so far, no distributed sensors with sapphire fibers have been reported in the literature. For distributed sensors with optical fibers, basically optical time-domain reflectometry (OTDR) or optical frequency domain reflectometry (OFDR)-based methods have been used. With those methods, best-achieved spatial resolution was around 1 meter. This means that those standard methods for distributed sensing can not be used for achieving centimeter spatial resolution, which is our case. Another method for distributed sensing is using fiber gratings such as fiber Bragg gratings (FBG) or long period gratings (LPG). Actually, these sensors are multiplexed sensors rather than distributed sensors because they don't provide continuous measurement along the fiber. By multiplexing several sensors, however, a few centimeters spatial resolution can be readily obtained, which has enough resolution in most cases. These 'quasi-distributed'sensors have high sensitivities, simple structures. Unfortunately, this grating-based method cannot be directly applied to sapphire fibers due to lack of photosensitivity of sapphire fibers. Micro-machining method might be a logical solution for gratings in sapphire fibers because the only way to perturb refractive index of the fiber without photosensitivity is to mechanically change the shape of the fiber.

1.2. Major Accomplishments

1.2.1 Set Up A Dedicated High Power, Ultrafast Laser System For Fabricating In-Fiber Gratings In Harsh Environment Optical Fibers

First, we have set up a dedicated high power, ultrafast (femto second) laser system for fabricating in-fiber gratings in harsh environment optical fibers (including the sapphire optical fiber), Fig. 2.

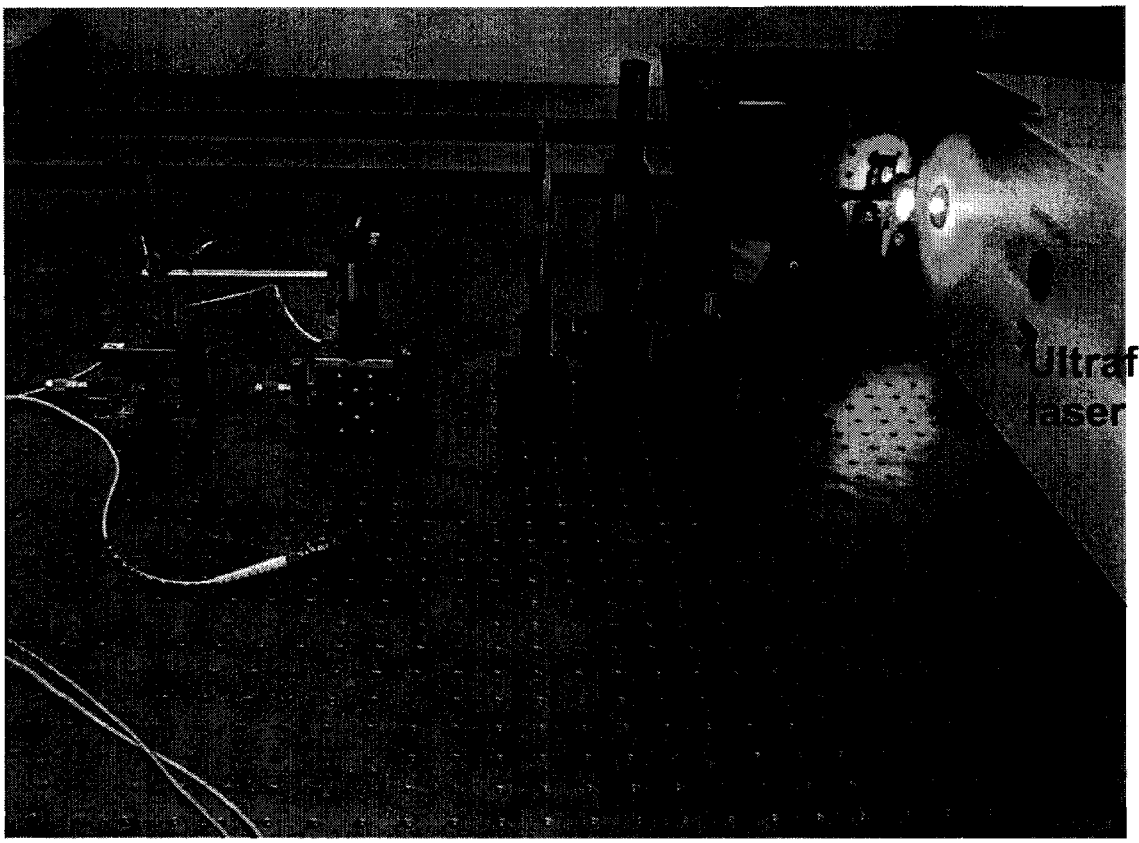

Figure 2. Ultrafast (femto second) experimental system for fabricating harsh environment fiber optic gratings.

1.2.2 Successfully Fabricating Gratings In Single Crystal Sapphire Fibers By The High Power Laser System

Second, we have successfully fabricated gratings in both silica and single crystal sapphire fibers by the ultrafast laser system, as shown in Fig. 3. The area with strong scattering light is the area with the grating. The diffraction pattern (upper right figure) clearly shows the grating diffraction pattern. Figure 4 shows the spectrum of the fabricated grating, which has an 8 dB peak with a spectral bandwidth around 1 nm, which is consistent with the theoretical data.

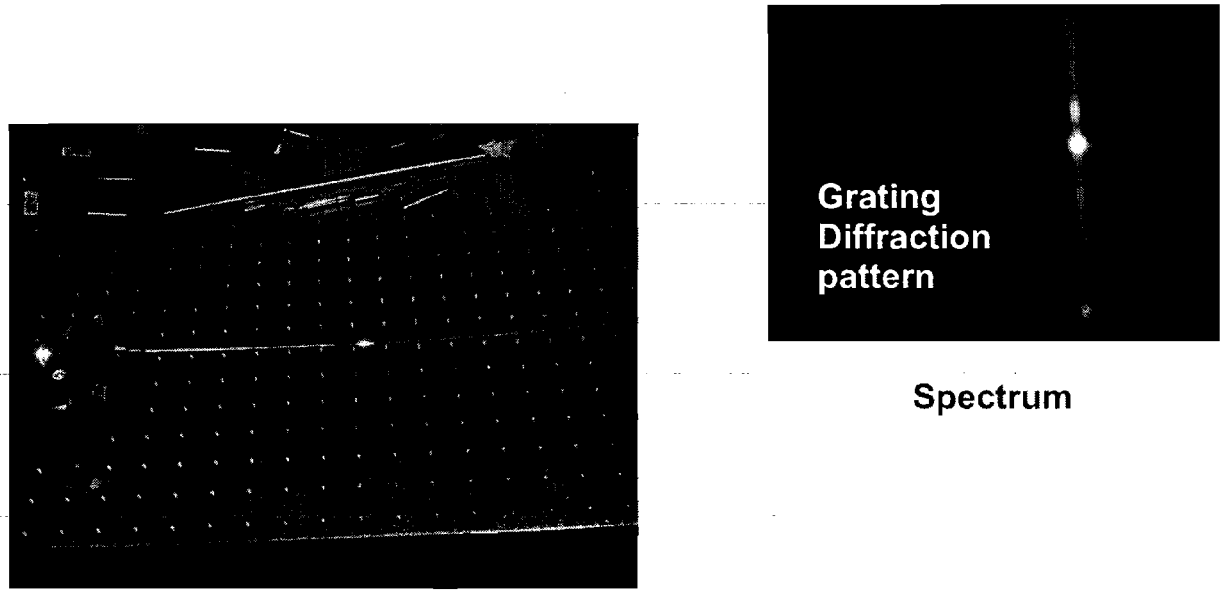

Figure 3. Fabricated gratings in single crystal sapphire fiber.

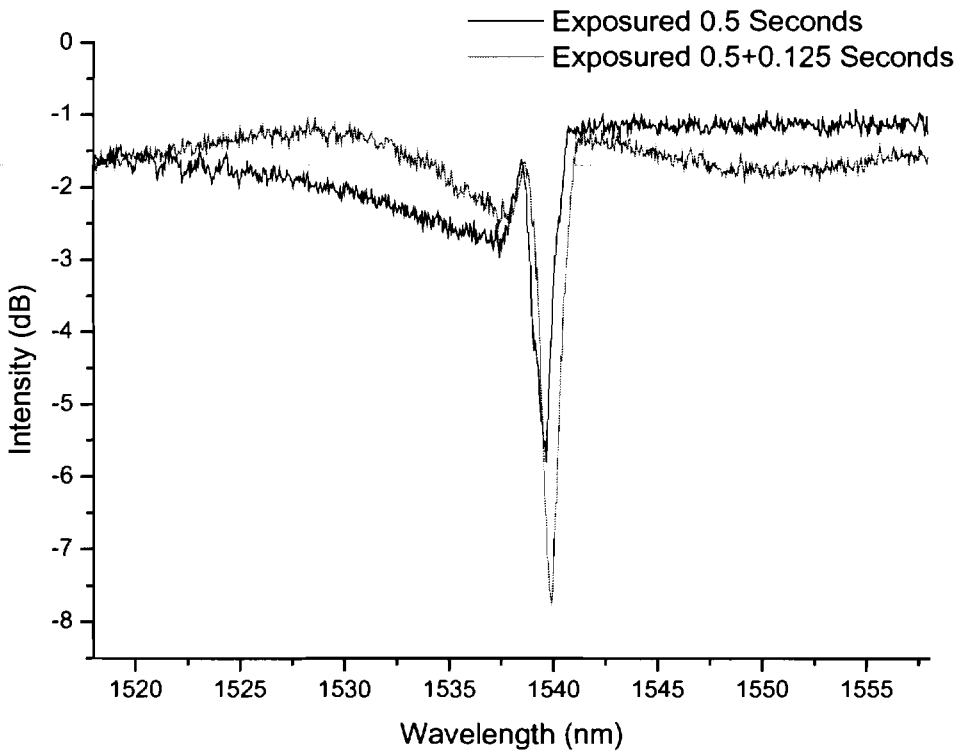

Figure 4. The spectrum of the grating fabricated by the ultra short laser pulses.

The major advantages of our approach are:

- We have successfully realized multiple gratings (six gratings in a single sapphire fiber), which is the key for the distributed sensing, as shown in Fig. 5.

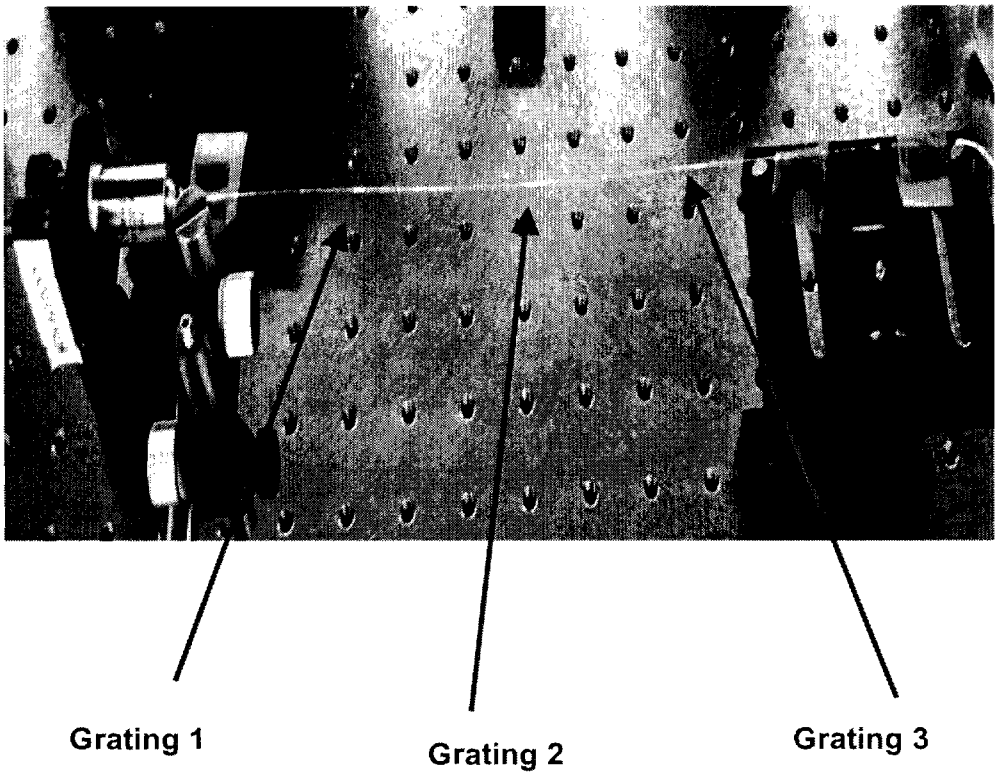

Figure 5. The multiple gratings fabricated in the same sapphire fiber.

- We have developed advanced gratings in single crystal sapphire fibers.
  - Ultra thin fiber (60 micron, regular 125 micron) (High coupling efficiency between this fiber and conventional silica fiber).
  - Advanced coupling with mode control (High grating quality).

We have performed initial reliability test on the grating (1400 °C). It survives at 1400 °C for 200 hrs. This demonstrates the reliability of this type of grating.

1.2.3 Develop highly sensitive long period gratings (LPG) by electric arc

Figures 6 (a) and (b) show the picture and corresponding drawing of electric arc grating fabrication system.

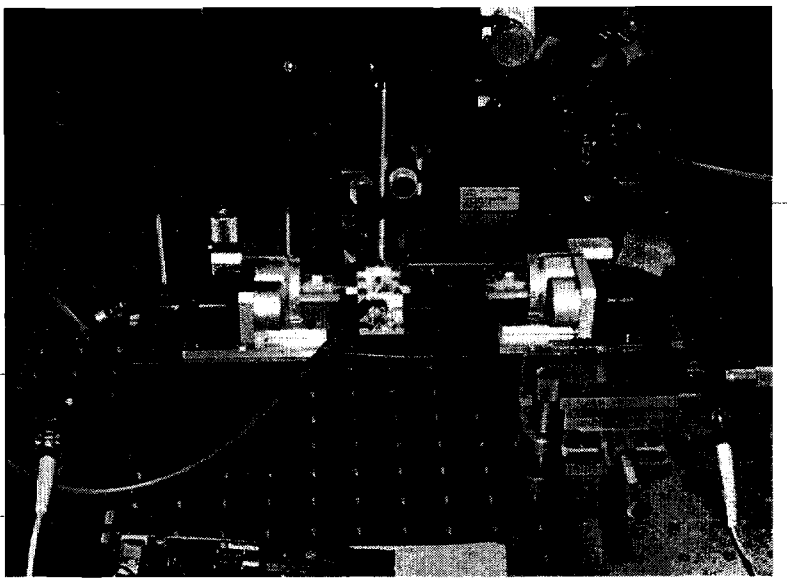

Figure 6 (a) A picture of electric arc grating fabrication system.

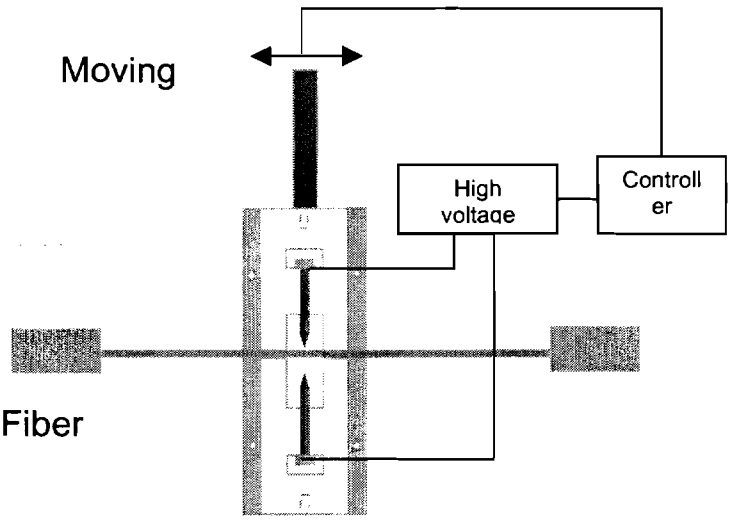

Figure 6 (b). Corresponding drawing of electric arc grating fabrication system.

A standard single mode communication fiber (SMF-28e) with a short unjacketed section was placed in two fiber holders. Both ends of the fiber were clamped by the holders and held straight. Two electrodes were mounted in a fixture that was moved by a nano-precision translation stage. The grating spectrum was monitored while the arc discharge was being produced. The entire fabrication process was fully controlled by a computer. Two methods have been used to fabricate LPFGs by electric arc discharge. The first creates micro-bends by introducing a small lateral displacement at one end of the fiber. The other tapers the fiber by attaching a mass to one end. Both methods induce refractive index modulation along with mechanical deformation. Depending on the position of the fiber in the arc flame and the applied stress to the fiber, the induced refractive index profile inside the fiber can be greatly affected, which in turn, affects the

coupling constant between core and cladding modes. For our experiment, the fiber sat in V-grooves made on the electrodes fixture. There was no lateral displacement at one end of the fiber, and no additional mass was attached. The arc current was ~ 15mA (RMS) with 20 kHz frequency, and the arc duration was changed while keeping arc current constant.

Figure 7 shows the evolution of a short LPFG as the number of arc discharges is increased. The arc duration was 357ms, and the period was 500μm for this grating. The resonant coupling rapidly grew and reached its deepest peak (-30dB) with 4 grating periods (5 arc discharge). The peak depth was reduced to -13.2dB with one more arc discharge due to over-coupling. The total grating length was 2mm when it reached the deepest peak. Using the measured peak depths, the number of periods, and the relation $t_{x,\max} = \sin^2(\kappa L)$, the coupling constant for this mode was estimated to be in the order of 10 cm^{-1}, which is over ten times larger than the typical coupling constant of LPFGs.

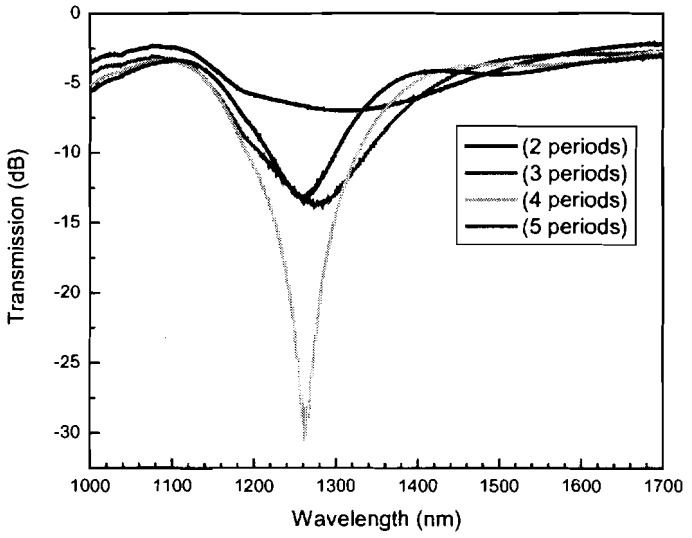

Figure 7. Evolution of the short arc-written LPFG.

For this short grating, a mechanical deformation was observed by an optical microscope as shown in Fig. 8. The magnitude of deformation was estimated to be approximately 10μm.

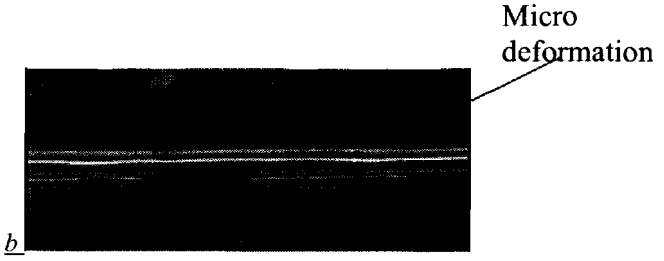

Figure 8. Optical microscope image of short arc-written LPFG.

1.3. Future Work Plan

We will test the fabricated harsh environment fiber optic gratings in the electric testing boiler available at the Energy Institute, Penn State University, in the year 2006.

1.4. Technical Publications

Refereed Journal Papers

1. Sung Hyun Nam, Chun Zhan, Jon Lee, Corey Hahn, Karl Reichard*, Paul Ruffin+, Kung-Li Deng++, and Shizhuo Yin, "Bend-insensitive ultra short long-period gratings by the electric arc method and their applications to harsh environment sensing and communication," Optics Express Vol. 13, pp. 731-737 (2005).
2. S. Nam and S. Yin, "High temperature sensing using Whispering Gallery Mode Resonance in bent optical fibers," IEEE Photonic Technology Letters, pp. 2391-2393 (2005).
3. Wei-Hung Su*, Kebin Shi, Zhiwen Liu, Bo Wang, Karl Reichard+, and Shizhuo Yin, " A large-depth-of-field projected fringe profilometry using supercontinuum light illumination," Optics Express Vol. 13, pp. 1025-1032 (2005).
4. Yi Yang, Jon Lee, Karl Reichard*, Paul Ruffin+, Frank Liang,++, Dave Ditto+++, and Shizhuo Yin, "Fabrication and implementation of a multi-to-single mode converter based on a tapered multimode fiber," Optics Communications, pp. 129-137 (2005).
5. Kun-Wook Chung and Shizhuo Yin, "Design of a tunable phase-shifted long period grating using partial etching technique," Microwave and Optics Technology Letters, pp. 18-21 (2005).

Refereed Conference Proceedings

1. B. Wang, J. Fu, Y. Liu, R. Guo, and S. Yin, "Vector sensing with electronic fiber speckle pattern interferometry," SPIE 5911, pp.59110O-1 – 59110O-10, San Diego, CA, August 1, 2005.
2. S. Yin, K. Deng, S. Nam, and K. Reichard, "Fiber optic high temperature sensing based on whispering gallery mode resonance," SPIE 5911, pp. 59110W-1 – 59110W-10, San Diego, CA, August 1, 2005.
3. F. Wu, Y. Yang, and S. Yin, "High precision fiber taper fabrication using the self-immersion depth control in chemical etching," SPIE 5911, pp.59110x-1 – 59110x-10, San Diego, CA, August 1, 2005.
4. Sung-Hyun Nam, Jon Lee, Shizhuo Yin, Karl Reichard, Paul Ruffin, and Qing Wang, "Ultrasensitive fiber optic sensors and their applications," SPIE 5691 pp. 120-128, San Jose, CA, 2005
5. Stuart (Shizhuo) Yin, Sung-Hyun Nam, Yi Yang, Chun Zhan, and Kun-Wook Chung, "Innovative Fiber Optic Gratings: Fabrications and Applications," Proceedings of

International Symposium on Advances and Trends in Fiber Optics and Applications, October 11-15, 2004, Chongqing University, Chongqing, China. (**Invited Paper**)

TASK 2: BOILER FURNACE MONITORING MODEL DEVELOPMENT

2.1 Objectives and Motivations

Development of the multi-dimensional combustion simulation model has been the focus of activities by Prof. Boehman and his student. The effort has primarily been to get a functional workstation, with CFD software, into place and to train the student on its application to multi-dimensional combustion simulation.

The graduate student has worked with a 2-D model of the Down Fired Combustor Modeling this boiler has provided the graduate student the opportunity to become skilled using FLUENT, to leverage existing grids and extensive prior experimental work for comparison. This represents a shift from the initial direction, which was to work on a 3-D simulation of the Demonstration Boiler. Subsequent applications of FLUENT will extend to the Drop Tube Reactor (DTR) and the Demonstration Boiler.

The student has become proficient at using Gambit 2.1.6, the grid generation software for FLUENT, in preparing the demonstration boiler grid for simulation. Specific skills include:

- discretizing grid volumes
- meshing complex geometries
- evaluating grid for skewness
- grid refinement
- creating mesh for data collection at desired spatial positions

The student has also acquired skills in FLUENT, specifically:

- prePDF generation (for combustion simulations)
- solver selection
- premixed & non-premixed systems
- steady state or transient simulations
- air-staging
- knowledge to carry out validation studies

2.2 Major Accomplishments

The hypothesis of this work is that a series of one dimensional, line-of-site temperature profiles will provide in-situ temperature information sufficient to predicting NOx emissions at the boiler exit, based on the degree of stratification within the combustor, and the relationship between stratification to NOx formation.

The desire to implement a temperature measurement-based monitoring and feedback control system for improved NOx control necessitates the discovery of a functional correlation between boiler temperature distributions, boiler operating parameters and NOx formation. This numerical modeling effort serves to determine how best to implement temperature profile information that can be obtained in real-time with a novel fiber optic sensor, which can provide a measurement of the temperature distribution along a line-of-site through the interior of the boiler. This work will be successful if information from 1D lines-of-site can be used to develop a numerical relationship between temperature and boiler exit NOx emissions, and that implementation of that

relationship provides unique exit NOx concentrations from the measured temperatures, for the group of temperature profiles from each case tested.

2.2.1 Relevant Mathematical Modeling Studies of NOx Formation in Practical Combustors

The motivation for this worked stemmed from low NOx burner design, which incorporates air staging, and produces unique temperature profiles within the boiler [1,2,3]. The referenced works showed evidence of temperature "signatures" within the boiler, resulting from stratified combustion within as a result of air-staging of inlet combustion air, as well as lower NOx emissions at the boiler exit compared to cases without air-staging.

Computational studies of a 3D model of an industrial sized boiler were carried out using FLUENT 6.1. Ratios of primary, secondary and tertiary air were varied per Table 1, and resulted in the tabulated exit NOx and temperatures. The parameters and models selected for these cases are consistent for each case, except for the ratios of secondary and tertiary air. Swirl was applied to the tertiary air stream.

Table 1. Boiler Air & Fuel Inlet Conditions and Resulting NOx & T at Boiler Exit.

	Case 1	**Case 2**	**Case 3**	**Case 4**
Primary Air	0.200	0.200	0.200	0.200
Secondary Air	0.200	0.375	0.550	0.725
Tertiary Air (swirled)	1.590	1.415	1.240	1.065
Fuel Flow Rate (kg/s)	0.17	0.17	0.17	0.17
T_{exit} (K)	1441	1523	1554	1617
NOx_{exit} (ppm)	164	527	837	924

Data was extracted from 12, 1D sensor locations throughout the boiler to be used for statistical analysis to determine a relationship between in-situ temperature measurements and exit NOx concentrations

In attempt to find a numerical correlation between temperature profiles within the boiler and exit NOx concentrations, or to provide proof of unique temperature profiles for each case, many relationships were studied. The first test involved running a series of tests in SAS/STAT with the ORTHOREG procedure. The series of tests are outlined in the appendices, and resulted in poor relationships, with R-squared values ranging from 0.01 to 0.6. Due to undesirable R-squared values, the relationships from these tests were dismissed. The statistical tests prove that there is no linear relationship between temperature and NOx along the 1D sensors within the boilers, for the given "lines" of data that were extracted.

In order to determine for sure whether any unique relationships between temperature(s) within the boiler and exit NOx exist, a series of statistical tests were completed. Note that the concentration of NOx at the boiler exit is as follows for Group B simulation cases: Case 1 < Case 2 < Case 3 < Case 4.

Though the in-situ boiler temperature measurements seem to provide no direct relationship with NOx at the boiler exit, temperature at the boiler exit and the corresponding NOx

concentrations were used in conjunction with air ratios for further statistical tests. For each case, area-averaged temperatures and NOx values from the boiler exit and tertiary air values were used to form a linear regression study in MiniTab. The results are shown in Equation 1, and show that exit temperatures and tertiary airflow values have a strong ability to predict exit NOx concentrations. In this equation, "Air" represents the amount of tertiary air entering the boiler, and "T" is temperature.

$$\text{NOx(ppm)} = -68 + 1.35T - 1050Air \qquad 1$$
$$\text{R-squared} = 94.5\%$$

The above regression study was repeated using the primary air values and the tertiary air values. This case reported the same regression equation and R-squared value. When substituting the values for secondary air for the tertiary air, a similar regression equation was reported, with an identical R-squared value.

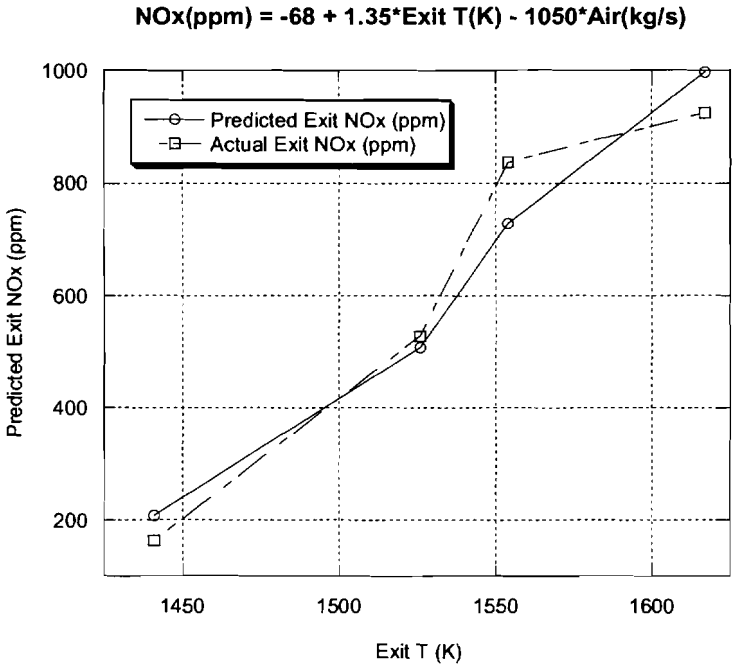

Figure 1. Exit NOx (ppm) Measured & Predicted vs. of Exit T(K)

Figure 1 depicts a plot of the actual NOx concentrations at the boiler exit, from simulations, as a function of temperature at the boiler exit, as well as the same trend achieved using the relationship from Equation 1. As the r-squared value of that equation indicates, the predicted trend relates closely to the simulated data.

The statistical analysis of of the computational data was evaluated using the following terms:

T_{avg} Average of temperatures from one sensor

ΔT_{avg}	The absolute difference between temperature values along one sensor, averaged over the number of differences calculated
Median	The middle number of a group of number arranged in ascending order
Std.Dev.	Standard deviation is the average amount by which values in a distribution differ from the mean value of that distribution
Variance	The square of the standard deviation value

Graphs representing the information described above are displayed below. Case 1 – Case 4 are indicated in the legend of each graph. T_{avg} values of the data for each sensor are shown in Figure 2 for all four data cases. Each case follows a consistent trend, with variations in temperature averages. Figure 3 shows the trends for ΔT_{avg}. For this statistical parameter, there is no consistent trend between cases for each sensor.

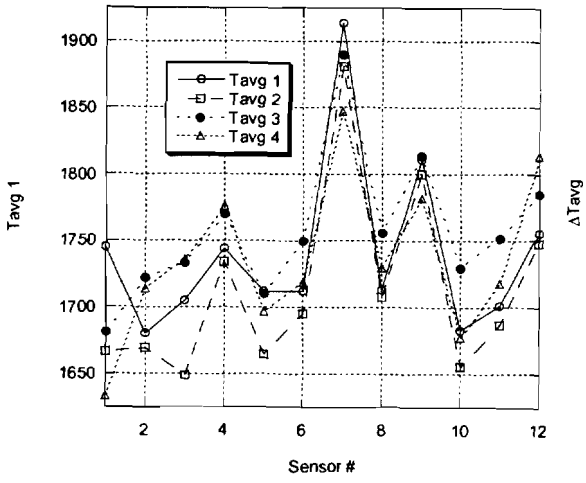

Figure 2. T_{avg} values for each sensor

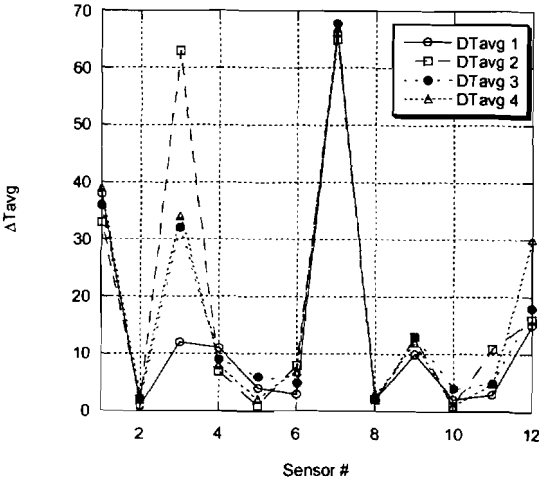

Figure 3. ΔT_{avg} values for each sensor

Trends for the median temperature of each sensor are shown in Figure 4, and provide no unique relationship between cases.

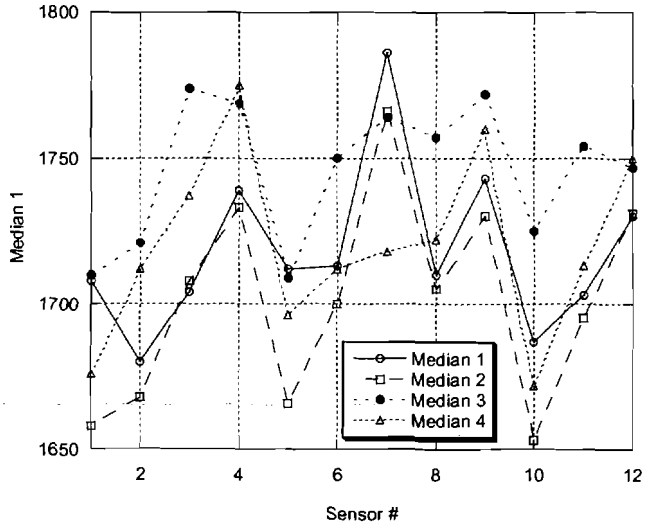

Figure 4. Median values for the temperatures of each sensor

Standard deviation and variance were also examined for data sets from each sensor, in hopes that the variation of temperature from one spatial location to the next may provide unique information in terms of temperature for each case. This idea was inspired by the work of Fiveland and Latham, and Epple, where temperature signatures for several cases were shown to be unique, as a result of air staging using low-NOx burners (2,3). Figure 5 portrays the standard deviation trends for all four cases, and Figure 6 contains variance plots. None of the curves produced for variance or standard deviation provide unique curves compared to the others within their data group.

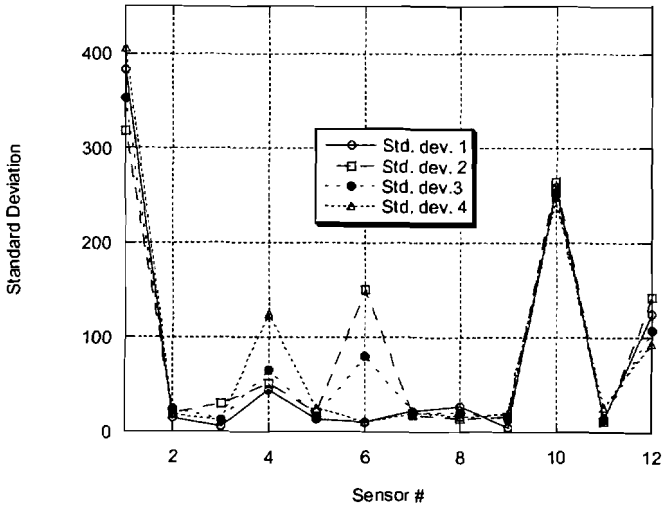

Figure 5. Standard deviation plots

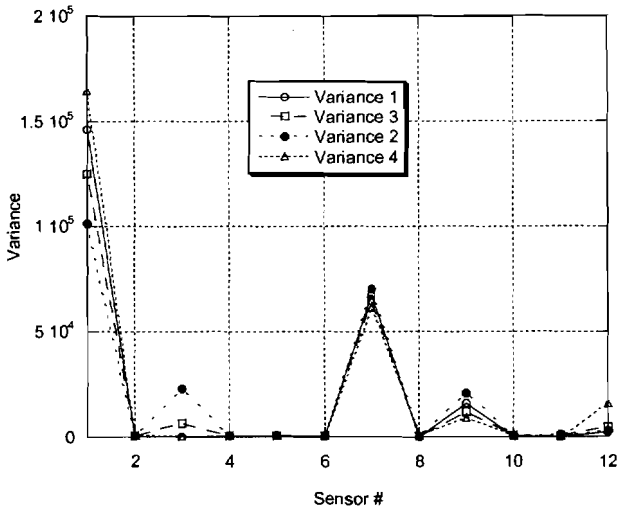

Figure 6. Variance plots

The overall finding of this investigation is that in-situ temperature measurements within a combustor are not sufficient to predict NOx emissions at the boiler exit. However, a regression study including tertiary air values and temperatures at the boiler exit show a good potential to predict exit NOx concentrations. It is important to note that the actual optical sensor would provide finer resolution in-situ temperature points than the rather course grid used in this study, and more lines of data (representing sensors) could be studied. Finer resolution in the numerical calculations may provide more distinct stratification to determine relationships between line-of-site temperatures and exit NOx emissions.

In order to improve and expand upon the results of this work, and to examine possibilities not investigated herein, it is proposed that the following studies be conducted:

- Validation study and stability analyses of the models employed.
- Mesh refinement studies of the existing grid, in order to assure the computational region appropriately represented the boiler, and to guarantee that the mesh spacing was adequate for detecting swirl and its effects. While a finer grid may be required to pick up the swirl effect, coarsening other areas of the grid where appropriate may save computational time.
- Improved combustion calculations, including a 2-stream PDF model, prompt NOx formation, and more accurate swirl representation.
- A comprehensive study of the behavior within the boiler, by examining temperature and flow fields for example, in order to determine the most appropriate spatial location for the 1D sensors.
- Determination of ability of a complex algorithm to link in-situ temperature information to exit NOx concentrations. The algorithm could survey the sensor

reading for the most stratification, and eliminate the temperature information outside the bounds of the stratified areas, and then use the selected information to look at possible correlations between temperatures and exit NOx.

- Investigation of an algorithm based on the occurrence of certain temperature values, or the frequency of series of temperature for a given sensor, may also be useful.
- Generate more data sets, perhaps a total of 10 or more, in order to improve upon the accuracy of the statistical relationships and tests performed in this work.
- Formulate statistical tests using the spatial information for each data point. Perhaps weighting certain data points due to their location can provide temperature information that to better link with exit NOx concentrations.
- The data from numerical calculations could be used with neural networks in order to determine exit NOx concentrations from in-situ temperature measurements.

2.3 Future Work Plan

The Demonstration Boiler, an industrial boiler located at Penn State's Energy Institute will be modeled using FLUENT and the 1D temperature measurement will be compared with the simulation. The 3D temperature distribution will be compared with the result of extrapolation by the system-type neural networks to be developed in Task 3 as an intelligent monitoring system for estimating temperature distribution in boiler furnace.

2.4 References

[1] R. Kurose, H. Makinob and A. Suzuki, "Numerical analysis of pulverized coal combustion characteristics using advanced low-NOx burner," *Fuel*, 2004. *In press.*

[2] B. Epple, R. Schneider, U. Schnell and K. hein, "Computerized analysis of low-nox coal-fired utility boilers," *Comb. Sci. Tech.*, 108, pp. 383-401, 1995.

[3] W.A. Fiveland and C.E. Latham, "Use of numerical modeling in the design of a low-nox burner for utility boilers," *Comb. Sci. Tech.*, 93, pp. 53-72, 1993.

TASK 3. INTELLIGENT MONITORING SYSTEM DEVELOPMENT

3.1 Objectives and Motivations

The proposed project will focus on an investigation of a mathematical approach to extrapolation, using a combination of system-type neural network architecture and the semigroup theory. The target of the investigation will be a class of distributed parameter systems for which, because of their complexity, lack an analytic description. Although the primary objective is extrapolation, this effort must begin with the development of an analytic description from the given empirical data, and then, proceed to extend that analytic description into an adjoining domain space for which there is neither data nor a model. That is, given a set of empirical data for which there is no analytic description, we first develop an analytic model and then extend that model along a single axis. Semigroup theory provides the basis for the neural network architecture, the neural network operation and also for the extrapolation process. Concerning the architecture, semigroup theory dictates that under certain circumstances, a given composite mapping should be regarded as two families of maps, requiring two separate neural network channels; concerning the operation, semigroup theory requires that the second channel possesses the classic semigroup property of mapping composition; concerning the extrapolation process, semigroup theory requires that the extrapolated elements share the same semigroup property that are possessed by the elements previously formed from the given empirical data. The semigroup theory provides a unified and a powerful tool for the study of differential equations on Banach space, covering system described by ordinary differential equations, partial differential equations, functional differential equations and combinations thereof [1]. For applications to control systems, estimation techniques are often required to compensate for an inadequate amount of data, arising from the unavailability of that data.

In the past, for systems described by ordinary differential equations, various estimation techniques have been developed with the most popular (and successful) ones being based on variations of the Kalman filtering theory. However, as control theory has been expanded to include more complex behavior, such as distributed parameter systems, described by partial differential equations, the estimation problem has taken on a new importance, because now it is necessary to provide estimated data at a great (theoretically infinite) number of points. A need therefore exists for a generalized estimation technique that can be applied to a broad class of nonlinear systems, any one of whose behavior is described by a partial differential equation. Stated very concisely, a need exists for a technique which can begin with a sparse set of data derived from a few discrete points within some continuum in one, two or three dimensional space and which can then develop estimated data at as many points as needed within the continuum, in a manner which is dynamically consistent with the given empirical data points, and additionally, to extrapolate the resulting function into an adjoining region of space for which there is no data.

The modeling technique uses a process referred to as algebraic decomposition to find a particular type of smooth approximating function to the empirical data, namely, one that lends itself to a representation as the product of a coefficient vector and a basis set of functions, where the coefficient vector possesses a semigroup property. Extrapolation involves only the coefficient vector and begins by training the semigroup channel neural network to replicate the coefficient

vector trajectory, while at the same time acquiring a semigroup property of its own (expressed in weight space). The acquisition of the semigroup property is dynamic, expressing itself as a particular sequence of weight changes. The learning algorithm is new in that the weight convergence is realized recursively, by training the neural network repetitively over successively longer intervals and searching for a second level of convergence. Extrapolation is concerned with discovering the dynamics of the weight change sequence and then autonomously continuing that sequence.

3.2 Development of Intelligent Monitoring System

Due to the difficulty and the delay of extracting accurate boiler furnace temperature data from FLUENT, the proposed method is applied to extrapolate enthalpy in a power plant to demonstrate the extrapolation capability as another example [2]. In this example, high temperature extrapolation is performed using proposed method.

3.2.1 Monitoring of Temperature Distribution in Boiler Furnace

The electric utility industry is charged to deliver power as inexpensively and as reliably as possible. Meeting these dual obligations has become increasingly difficult over the past 30 years. Environmental and economic concerns pressed the utility industry to develop clean and efficient ways of burning coal and oil. This has required major improvements in instrument, data management, and control of electric power plant components such as boilers. It has become a challenge to measure high temperature distributions of high-pressure liquids, steam, combustion gases, and heat transfer components in extremely adverse power plant environments. Traditional sensors have not exhibited sufficient stability and long-term accuracy without requiring expensive maintenance and recalibration. Additionally, each sensor only provides one reading so that only a limited number of readings are obtained.

Fig. 1 in Task 1 shows the Penn State down-fired combustor (DFC), which is an advanced pilot-scale furnace designed to evaluate the combustion performance of various fuels (natural gas, coal, coal-water slurry fuel) including emissions monitoring. The combustor has a 20-inch internal diameter, is 10 feet high, and is designed for a thermal input of 350,000 Btu/h (nominal), but this can be varied from 200,000 to 500,000 Btu/h. The proposed boiler furnace-monitoring model addresses the estimation of spatial temperature distribution continuously for any operating condition.

As an alternative to the above model-based estimation techniques, such as infinite dimensional extended Kalman filtering, an intelligent monitoring scheme will be developed for 3D temperature estimation by using the proposed system-type neural networks [3]. An intelligent algorithm will be developed to adaptively tune the monitoring system in real-time to implement in the experimental boilers. The previous emphasis on the application of computational intelligence for control and diagnostic will be shifted to state estimation and prediction problems.

3.2.2. Extrapolation of Enthalpy in a Power Plant

The electric utility industry is confronted with the task of estimating the steam enthalpy at various points in the water-steam cycle in a power plant. The two prominent estimation points are at the boiler, where water is converted into steam, and also in the delivery section which precedes the turbine where the energy of the steam is extracted and converted into mechanical power. It is very important to have functions which are able to accurately describe the correlations between enthalpy and temperature for the water/steam because the enthalpy provides the best description of the energy content for a compressible gas. In the literature, there are numerous works which present mathematical functions of enthalpy vs. temperature, but in many cases they provide insufficient approximation with experimental data or have a good approximation only over a small temperature range [4]. In addition, these methods have no provision for extending (extrapolating) accurate readings into a higher temperature range in which the readings become questionable. In this research, a new method of extrapolating the enthalpy is proposed using a system-type neural network architecture. Essentially, rather than relying on questionable temperature readings to calculate the enthalpy, this method extrapolates a set of reliable enthalpy readings directly.

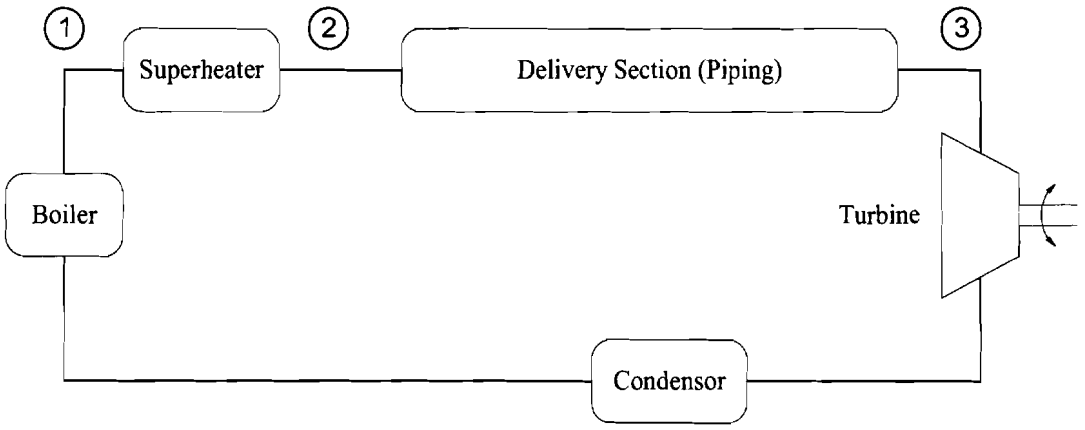

Fig. 1. General Power Plant.

Considering the general power plant as shown in Fig. 1, and referring to the delivery section from points 2 to 3, which precedes the turbine in a power plant, there is a need for tracking the steam enthalpy, since it is this function which ultimately determines the mechanical power delivered by the turbine. From the conservation of energy principle, the turbine work per mass of airflow is equal to the change in the enthalpy of the flow from the entrance to the exit of the turbine. Therefore, if we can measure the enthalpy among the delivery section and turbine, we can determine the mechanical power which then becomes the electrical power. The difficulty is that the enthalpy is derived from the temperature and, in the usual cases, these involve very high temperatures, and accurate readings of high temperature steam in the presence of high pressures are very difficult to achieve. At present, various temperature compensation schemes are employed but, even with these, the resulting temperature readings are questionable. Therefore, the resulting enthalpy estimations are questionable [5]. The proposed method suggests an alternative, namely, to obtain a small (sparse) set of reliable temperature-pressure readings at the

front end of the delivery section, forming the enthalpy from those readings, and then extrapolating those enthalpy readings directly.

3.2.3. Failures/shortcomings of Conventional ANN's

Recently, a shift has occurred in the overall architecture of neural networks from simple or component-type networks to system-type architectures. The most popular architecture seems to be the one advocated by Jacobs and Jordan [6], called the "Modular Connectionist Architecture", one example of which is shown in Fig. 2 [7]. It consists of a collection of expert components, each being trained independently, tied together by a component called the "gating logic" element, whose function is to decide on the relative contributions to be made by each expert component, such that when they are added, they provide the correct output for a given input. The present proposed method represents an adaptation of Fig. 2.

The most serious flaw in the design of system-type neural networks is the lack of a cohesive discipline in the architectural design and in the design of the learning algorithm. Virtually, the entire design is done on an intuitive basis. As a contrast to intuition, the proposed method relies on semigroup theory for the design of the semigroup channel.

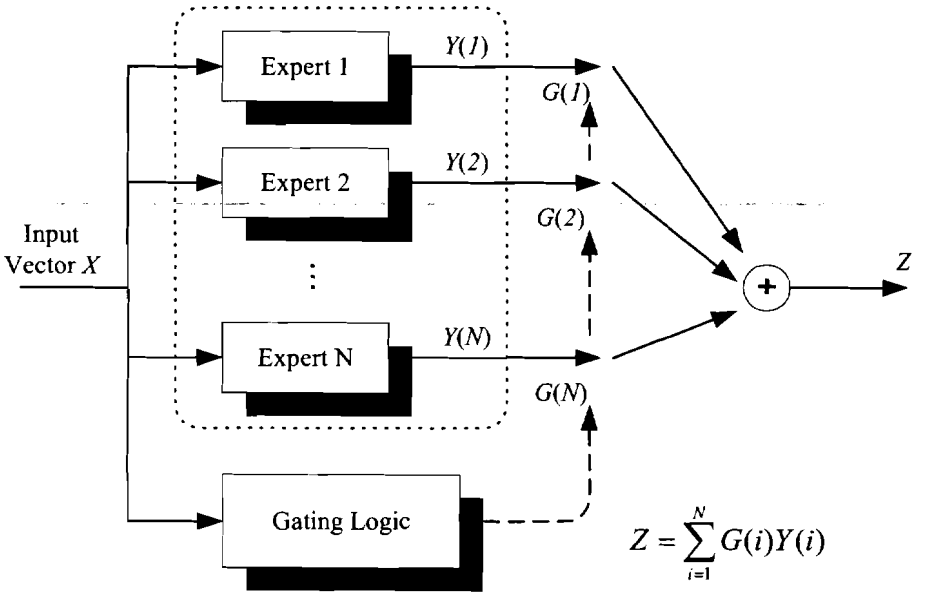

Fig. 2 Modular connectionist architecture.

To illustrate the lack of a cohesive discipline, in [7], the partitioning of components corresponds to separation of variables, which works if the variables are separated and does not work if the variables are not separated.

3.2.4 Proposed Neural Network Architecture

Neural networks are being used for systems described by PDE's [10]. The system-type attribute of the neural network architecture is shown in Fig. 3, implementing an arbitrary function $T(z,r)$. Unlike conventional neural network architectures that would attempt to achieve the mapping $T(z,r)$ with one neural network, the proposed architecture reflects a system-type approach using two neural network channels, a Function Channel and a Semigroup Channel, in an adaptation of the connectionist architecture (Fig. 2). During use, the semigroup channel supplies the function channel with a coefficient vector $C(z)$ as a function of the index z. The coefficient vector, when applied to the basis set $E(r)$ of the function channel, causes the function channel to operate as one specific function from within a vector space of functions. Jointly, these two channels realize a semigroup-based implementation of the mapping $T(z,r)$. The similarity between the proposed architecture (Fig. 3) and that of Fig. 2 arises from the fact that the Function channel is implemented as N "expert" systems.

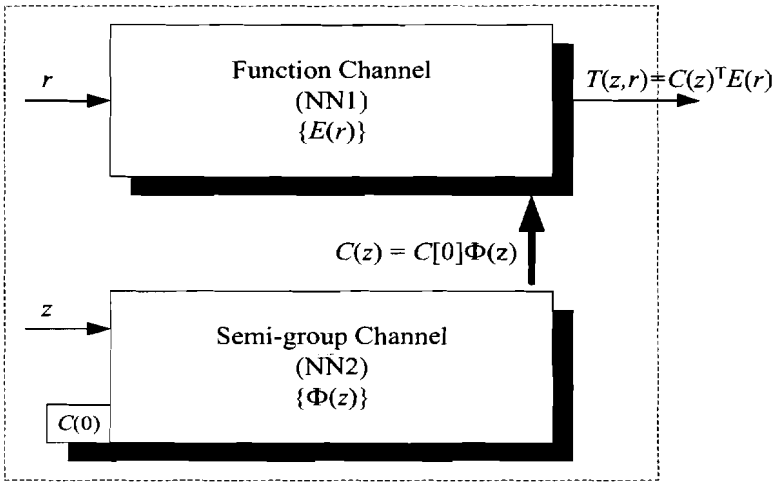

Fig. 3. System-type architecture.

The function channel can have a Radial Basis Function (RBF) architecture [11]. It consists of n RBF networks, each one of which implements one orthonormal vector of an n-dimensional basis set of vectors $E(r)$. The outputs of the orthonormal vectors are (internally) linearly summed so that the channel spans an n-dimensional function space. The coefficients which determine the linear sum and thereby define the specific function being implemented is supplied by the semigroup channel. Up to this point, the operation of the RBF channel parallels the idea used by Phan and Frueh [12]. One of the essential differences between their approach and the present proposed approach is that the former requires prior engineering knowledge for selecting the basis vectors, and the latter approach requires no such knowledge. One advantage that RBF networks have over other architectures is that their functionality can be given an explicit mathematical expression in which the neuron activation functions act as Green's functions [13], [14]. This makes these networks amenable to design rather than training. Another advantage is that they function as universal approximators [11]. The semigroup channel can be adapted from the Diagonal Neural Network (DRNN) [15], [16] or the Simple Recurrent Network (SRN)

architecture [17], in which the input is split into a dynamic scalar component z and one static vector component, the vector $C(0)$. The output is a vector $C(z)$, which is related to the dynamic input z and to the static input $C(0)$ by the semigroup property: $C(z) = \Phi(z)C(0)$, where $\Phi(z_1 + z_2) = \Phi(z_1)\Phi(z_2)$. (Refer to Fig. 3).

3.2.5 Learning Algorithm of Proposed System-type NN

The first component of the system, namely the Function Channel, since it is composed of RBF components, can be designed, rather than trained. The second component, the Semigroup Channel, can be trained in the new way illustrated below. During training, the semigroup channel receives as input a preliminary coefficient vector $C(z)$ and produces a smoothened coefficient vector $\tilde{C}(z)$. That is, the primary objective of training is to replicate (and, if necessary, to smoothen) the vector $C(z)$ with a vector $\tilde{C}(z)$ which has the following semigroup property [18]: $\tilde{C}(z) = \Phi(z)\tilde{C}(0)$, where $\tilde{C}(z) \equiv [\tilde{c}_1(z), \tilde{c}_2(z), ..., \tilde{c}_n(z)]^T$ and $\Phi(z)$ is an nxn matrix that satisfies: $\Phi(z_1 + z_2) = \Phi(z_1)\Phi(z_2)$. However, there is a secondary objective of training; the channel must also "replicate" the semigroup property of the trajectory by gradually acquiring a semigroup property of its own, in weight space. The existence of this acquired semigroup property in weight space becomes the basis for extrapolation. In order to elicit this gradual acquisition of the semigroup property, it is necessary that the training in this second step (semigroup tracking) occur in a gradual manner, as shown in Fig. 4. In Fig. 4, the entire trajectory is split into successively-longer sub-trajectories.

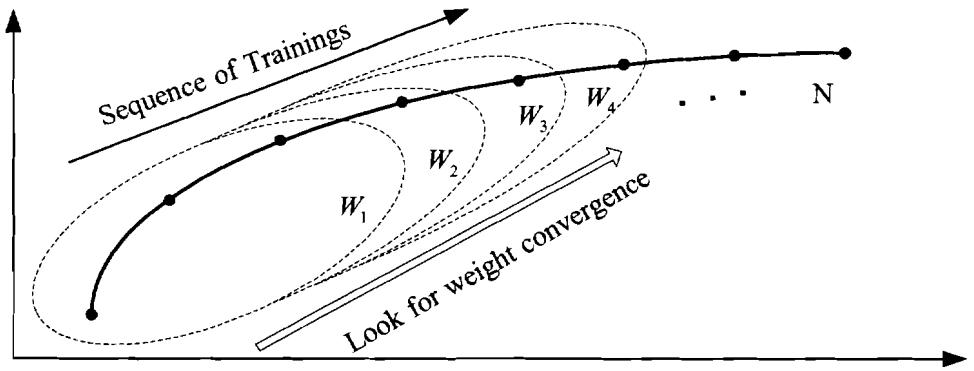

Fig. 4. Overview of new training algorithm.

It must be noted that there are two concepts of convergence that occur. First, to acquire a given weight, for example, weight W_3, requires conventional training convergence, which in turn may require 500 training iterations. Second, after all weights (W_1, W_2, ..., W_n) have been obtained, a search begins for a convergence within this weight stream alone. Extrapolation involves only the coefficient vector and the SRN network (the semigroup channel). At the uppermost level, the idea is to train the neural network to replicate the coefficient vector (produced by the previous system modeling effort) in such a way that it is additionally

replicating the semigroup property, which is responsible for generating the coefficient vector by acquiring a semigroup property of its own in weight space. As a comparison, some other recent extrapolation attempts are given in [19]. One current method, which also attempts to build a universal framework for extrapolation, occurs in various forms in nonlinear control theory and is collectively called "continuation methods." These methods have been in existence for some time, but are only recently receiving attention [20].

3.3 Simulation and Estimation Results

3.3.1 Monitoring of Temperature Distribution in Boiler Furnace

The following illustrates simulation results of the application of the proposed method to the prediction (extrapolation) of temperature data from a boiler furnace of dimensions comparable to that found in a power plant. The data represents "raw data" furnished by the Penn State Energy Institute. The geometry of the furnace is cylindrical with the z-axis along the furnace axis, and with r going from one wall to the other wall. (Note that r is a diameter, not a radius.) A simulation will be performed on the configuration below, where there are 25 probes, each one providing 11 readings. The extrapolation will be simulated in the region occupied by probes 25 to 30, Fig. 5. The results of the extrapolation will be compared to given raw data in that region. The temperature distribution is shown in Fig. 6.

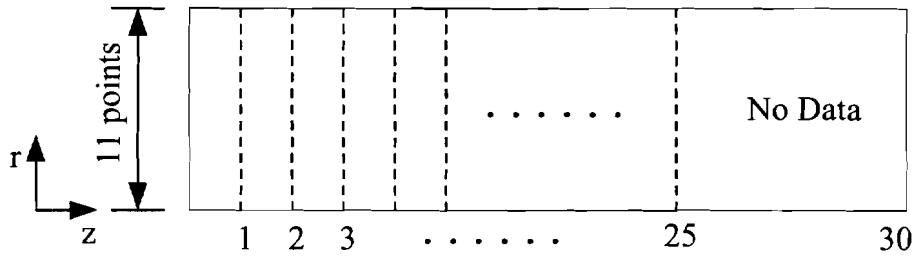

Fig. 5. Temperature probe configuration for the furnace.

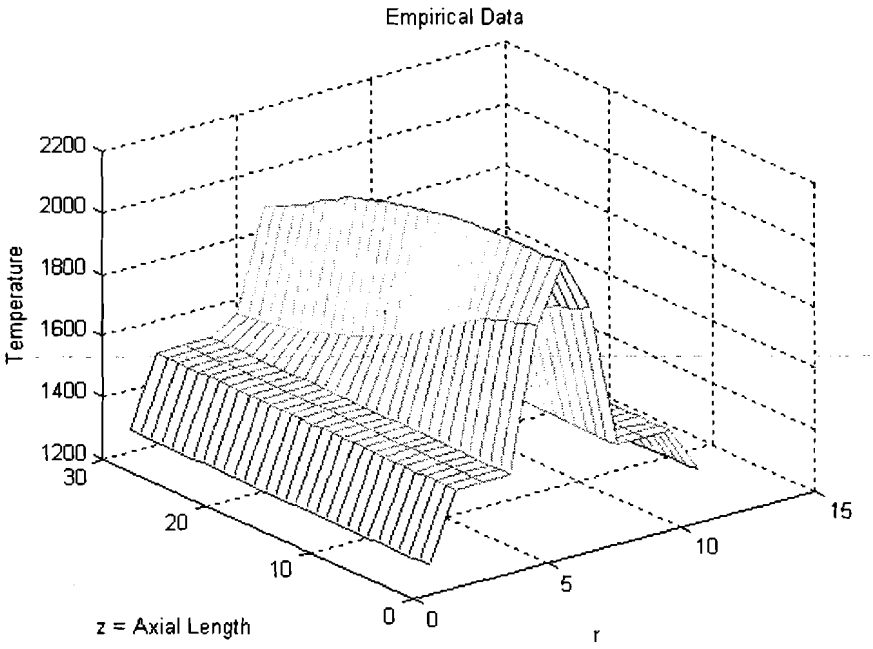

Fig. 6. Temperature distribution for the furnace.

The preliminary (rough) coefficient vector produced by the RBF network are shown in Fig. 7. The use of this rough coefficient vector together with the basis set of vectors can produce the computed temperature distribution shown in Fig. 8.

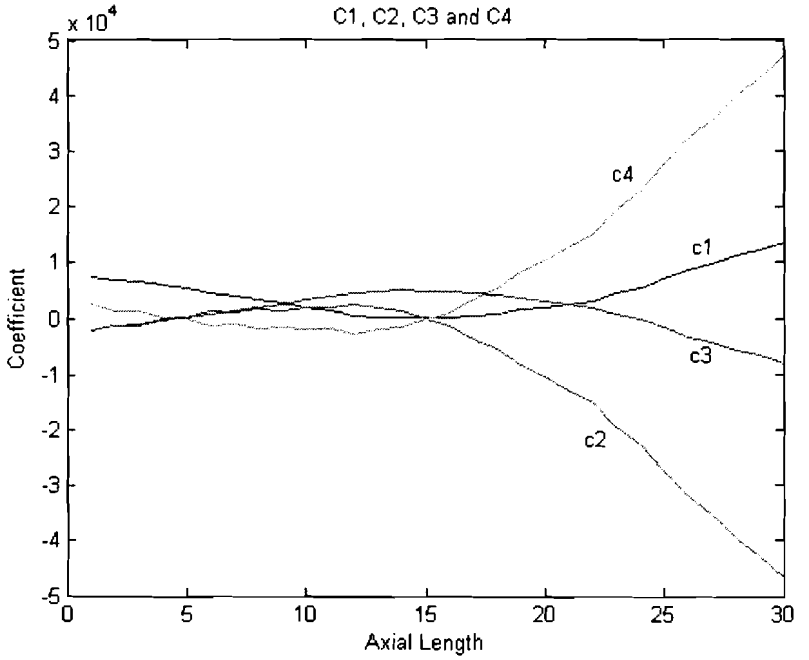

Fig. 7. Preliminary coefficient vector set.

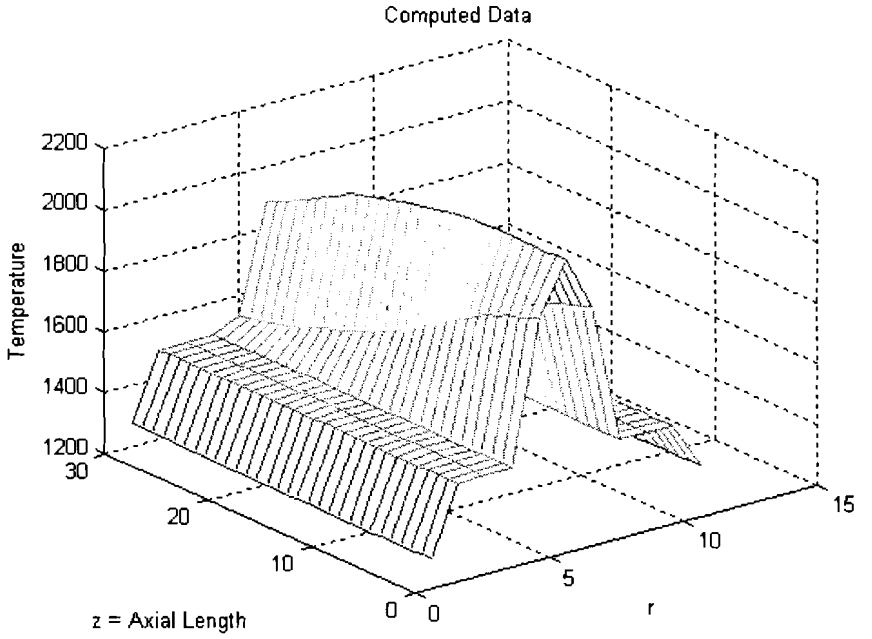

Fig. 8. Computed temperature.

The possibility for extrapolation begins by checking for weight convergence as training is performed along the coefficient vector. In this case, weight convergence occurs as this training is repeated over successively longer intervals (refer Fig. 4). It is this weight convergence, which becomes the basis for extrapolation. In this case, because of the smoothness, the possibility for extrapolation exists and the next step is to apply an extrapolation test in which the trailing end of the weight change sequence (produced by training) is replaced by an equivalent weight change sequence based on a rule that generates a semigroup. Based upon an observation of the weight change sequence on the interval from 15 to 20, a semigroup-based rule for weight change is formulated and applied to the interval from 20 to 25, as a test. Extrapolation (to the region where no data were assumed) consists of the autonomous continuation of the rule for weight change, which was derived during the extrapolation test. These results are shown in Fig. 9 below (only the first two coefficients are shown).

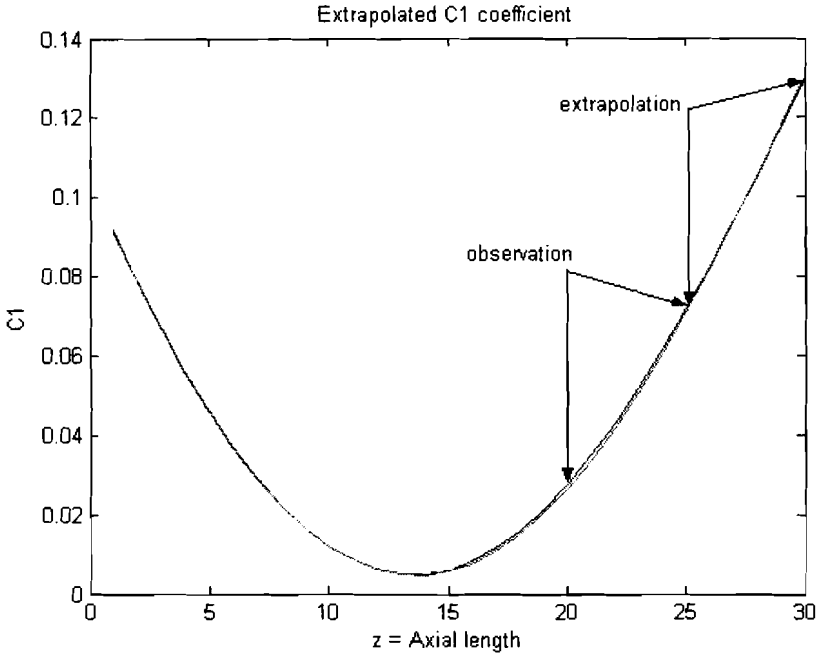

Fig. 9a. Extrapolation results for C1.

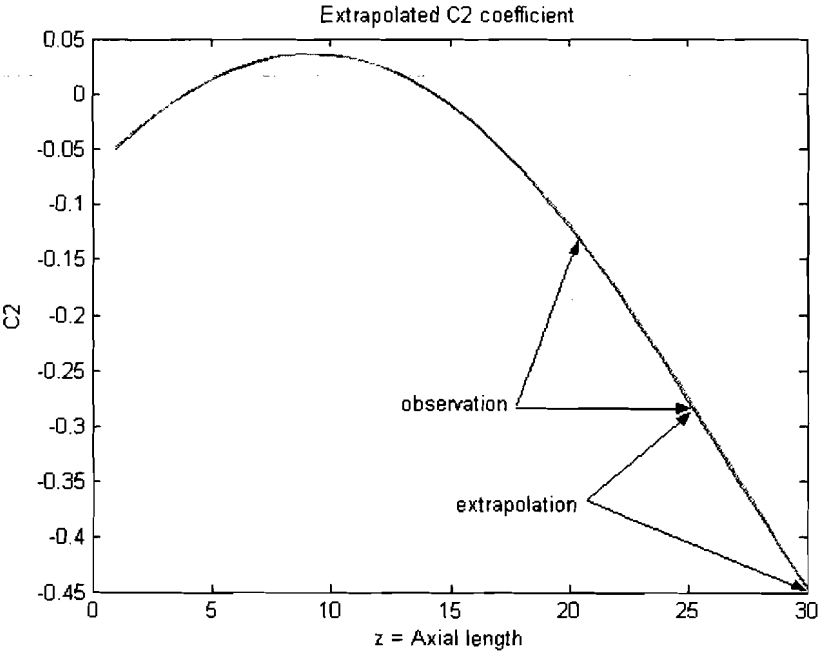

Fig. 9b. Extrapolation results for C2.

3.3.2. Demonstration of Extrapolation Capability for Enthalpy in a Power Plant

3.3.2.1 Water Enthalpy

The water enthalpy data corresponding to the temperature and pressure is obtained from the NIST Chemistry WebBook [21]. The range of temperature is 100°F to 400°F and the range of pressure is 300 psi to 2300 psi. Although the preferred method of extrapolation in this case would be along the temperature axis, it is now demonstrated that the proposed method can be applied to the pressure-extrapolation of the enthalpy of water for temperature-pressure distributions which typically exist in the power plant at the exit of the boiler (wet stream – point 1 in Fig. 1). The water enthalpy is first re-expressed as the vector product: $h(T,P) = C(P)E(T)$ and extrapolation is performed along the pressure axis. Fig. 10 displays the error between the given empirical enthalpy and the computed enthalpy; Fig. 11 displays the smoothened coefficient vector and Fig. 12 displays the extrapolated coefficient vector. Based upon an observation of the weight change sequence on the interval from 1500 psi to 1750 psi, a semigroup-based rule for weight change is formulated and applied to the interval from 1750 psi to 2000 psi, as a test. Extrapolation consists of the autonomous continuation of the rule for weight change, which was derived during the extrapolation test. Extrapolation is performed from 2000 psi to 2300 psi where no data were assumed based on the observation which is previously test region.

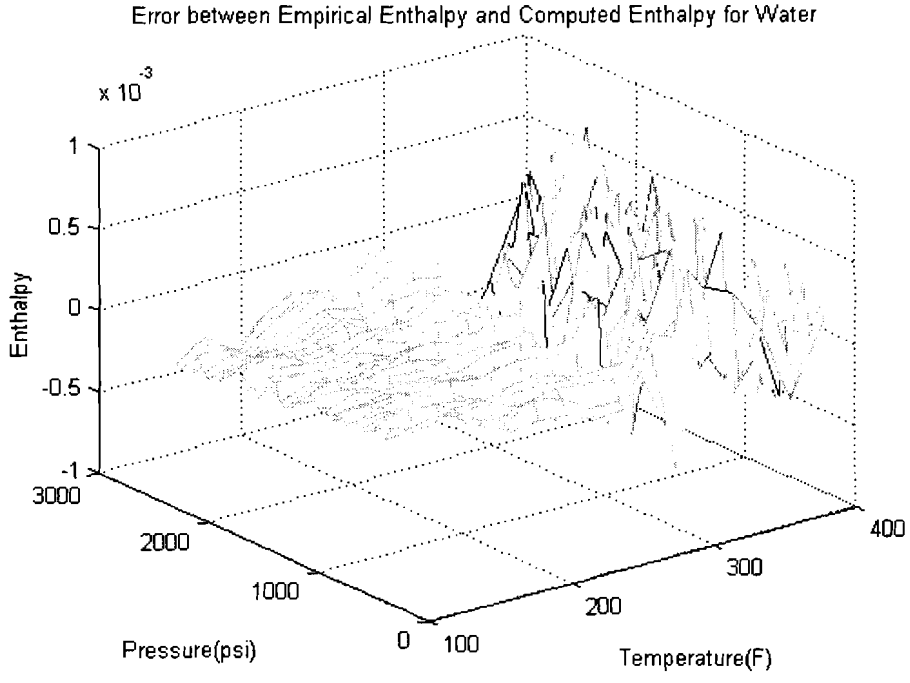

Fig. 10. Error between empirical and computed enthalpies.

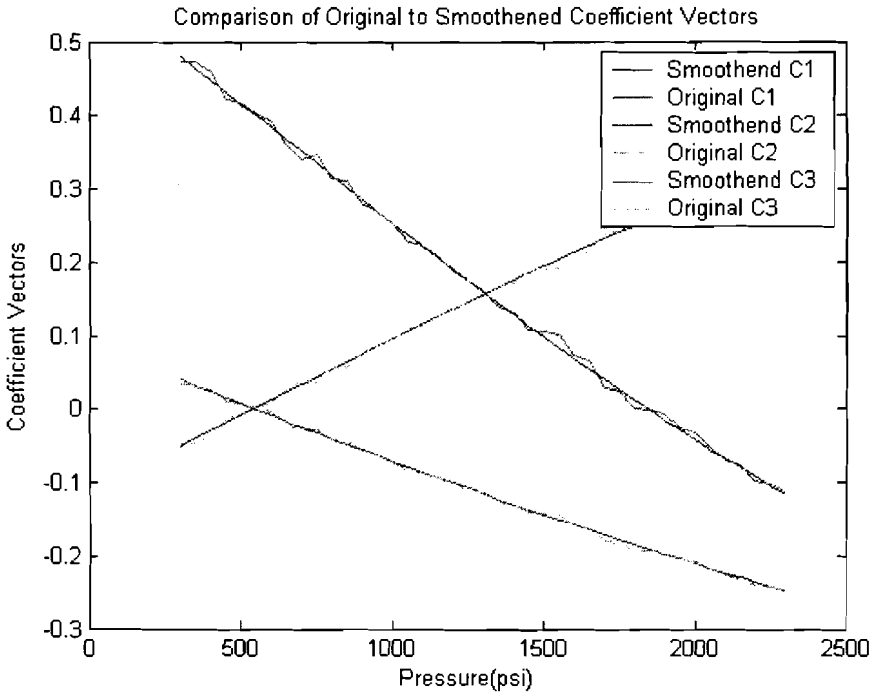

Fig. 11. Smoothened coefficient vectors.

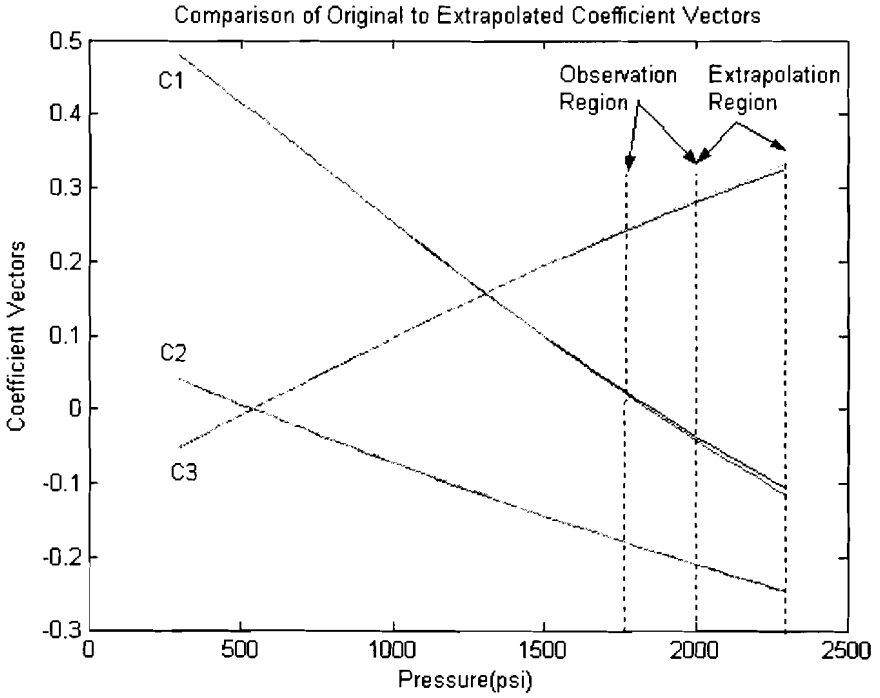

Fig. 12. Extrapolated coefficient vectors.

3.3.2.2 Steam Enthalpy

The steam enthalpy corresponding to the temperature and pressure is obtained from the NIST Chemistry WebBook [21]. The range of temperature is 800°F to 1200°F and the range of pressure is 800 psi to 1500 psi. The proposed method will now be applied to the extrapolation of the enthalpy of steam for temperature-pressure distributions which typically exist in the power plant after the water has exited the boiler and the superheater and travels through the delivery section to the turbine (dry stream – points 2 to 3 in Fig. 1). The steam enthalpy is first re-expressed as the vector product: $h(T,P)=C(P)E(T)$ and extrapolation is performed along the temperature axis. (Among other things, this also demonstrates that, in certain cases, extrapolation can be performed in more than one way.) Fig. 13 displays the error between the given empirical enthalpy and the computed enthalpy; Fig. 14 displays the smoothened coefficient vector and Fig. 15 displays the extrapolated coefficient vector. Based upon an observation of the weight change sequence on the interval from 1040°F to 1090°F, a semigroup-based rule for weight change is formulated and applied to the interval from 1090°F to 1140°F, as a test. Extrapolation consists of the autonomous continuation of the rule for weight change, which was derived during the extrapolation test. Extrapolation is performed from 1140°F to 1200°F where no data were assumed based on the observation which is previously test region.

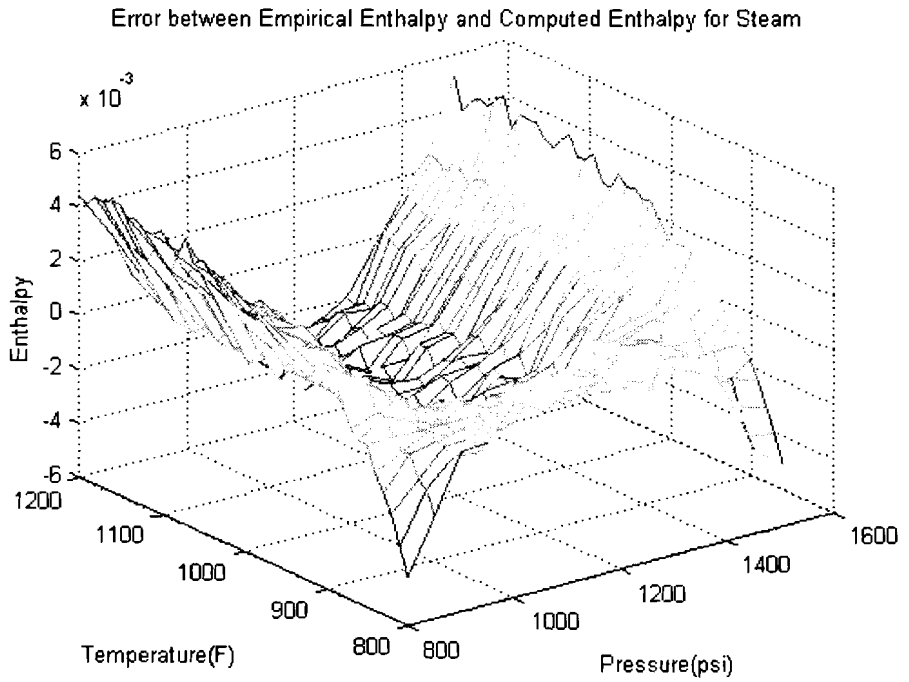

Fig. 13. Error between empirical and computed enthalpies.

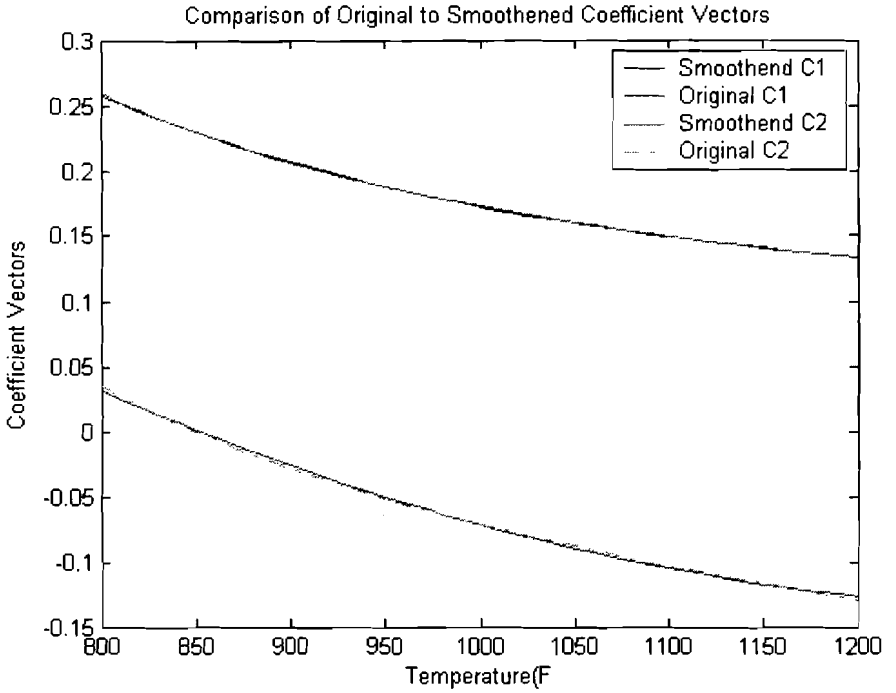

Fig. 14. Smoothened coefficient vectors.

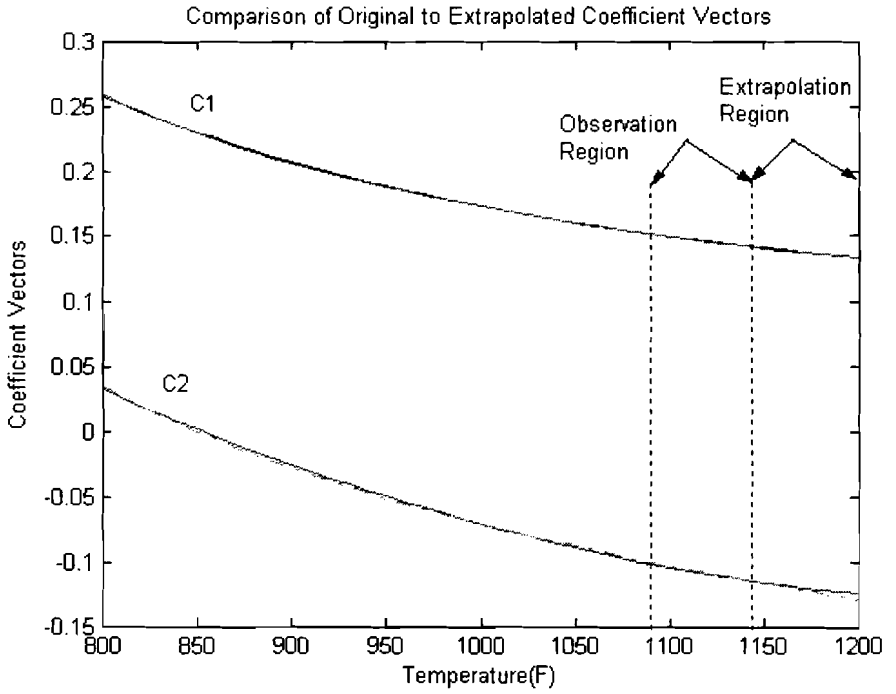

Fig. 15. Extrapolated coefficient vectors.

3.4. Conclusions

In this research, we investigate a mathematical approach to extrapolation of the temperature distribution within a power plant boiler facility and enthalpy in a delivery section within a power plant, using a combination of a modified neural network architecture and semigroup theory. Given a set of empirical data with no analytic expression, we first develop an analytic description and then extend that model along a single axis. This can be achieved by using the algebraic decomposition to obtain an analytic description of empirical data in a specific form, called the semigroup form, which involves the product of a coefficient vector and a basis set of vectors. If this form can be achieved, the describing aspect is simplified because the description of the coefficient vector is decoupled from the description of the basis vector. Additionally, each component of the coefficient vector and each component of the basis set of vectors can be described individually. From the results, we conclude that the proposed system-type neural network architecture works well both temperature and enthalpy extrapolation.

3.5 Future Work Plan

The concept of the system-type neural networks will be applied to develop an intelligent monitoring system for estimating temperature distribution in boiler furnace.

3.6 References

[1] K. Li and S. Thompson, "A cascaded neural network and its application to modeling power plant pollutant emission," *Proceedings of the 3rd World Congress on Intelligent Control and Automation*, pp. 992–997, Vol. 2, 28 June-2 July 2000.

[2] B. H. Kim, J. P. Velas, and K. Y. Lee, "Semigroup based neural network architecture for extrapolation of enthalpy in a power plant," *Proceedings of the ISAP*, pp. 291-296, 2005.

[3] K. Y. Lee, J. P. Velas, and B. H. Kim, "Development of an intelligent monitoring system with high temperature distributed fiberoptic sensor for fossil-fuel power plants," *IEEE Power Engineering Society General Meeting*, pp. 1350-1355, Jun 6-10, 2004.

[4] R Lanzafame and M. Messina, "A new method for the calculation of gases enthalpy," *Energy Conversion Engineering Conference and Exhibit*, vol.1, pp. 318~328, July 2000.

[5] M. A. Tahani and C. Lucas, "Development of expert controller for steam temperature regulation in power plants," *IEEE/RSJ International Workshop on Intelligence for Mechanical Systems*, vol.3, pp. 1333 – 1337, Nov. 1991.

[6] R. Jacobs and M. Jordan, "A competitive modular connectionist architecture," *Advances in Neural Information Processing Systems*, Vol. 3, pp. 767-773, Morgan-Kaufmann, Cal., 1991.

[7] Atiya, R. Aiyad, and S. Shaheen, "A practical gated expert system neural network," *IEEE International Joint Conference on Neural Networks*, Vol. 1, pp. 419-424, 1998.

[8] N. U. Ahmed, *Semigroup theory with applications to systems and control,* Longman Scientific & Technical, Harlow, 1991.

[9] H. Tanabe, *Equations of Evolution*, Pitman Publishing Ltd., London, 1979.

[10] R. Padhi and S. N. Balakrishnan, "Proper orthogonal decomposition based feedback optimal control synthesis of distributed parameter systems using neural networks,"

Proceedings of the 2002 American Control Conference, 2002, pp. 4389–4394, Vol. 6, pp. 8-10, May 2002.

[11] S. Haykin, *Neural Networks,* 2nd ed., Prentice Hall, N.J., 1999.

[12] M. Q. Phan and J. A. Frueh, "Learning control for trajectory tracking using basis functions," *Proceedings of the 35th IEEE Conference on Decision and Control*, pp. 2490-2492, Dec. 1996.

[13] A.N. Tikhonov, "On regularization of ill-posed problems," *Doklady Akademii Nauk USSR,* vol. 153, 1973.

[14] A.N. Tikhonov, "On solving incorrectly posed problems and method of regularization," *Doklady Akademii Nauk* vol. 151, USSR, 1973.

[15] C. C. Ku, K.Y. Lee, and R.M. Edwards, "Improved nuclear reactor temperature control using diagonal recurrent neural networks," *IEEE Trans. on Nuclear Science*, Vol. 39, pp. 2298-2308, December 1992.

[16] C. C. Ku and K.Y. Lee, "Diagonal recurrent neural networks for dynamic systems control," *IEEE Trans. on Neural Networks,* Vol. 6, pp. 144-156, January 1995.

[17] J. Elman., "Finding structure in time," *Journal of Cognitive Science*, Vol. 14, pp. 179-211, 1990.

[18] Miyadera, *Nonlinear Semigroups*, American Mathematical Society, Providence, R.I., 1992.

[19] Z. Altman and R. Mittra, "A technique for extrapolating numerically rigorous solutions of electromagnetic scattering problems to higher frequencies and their scaling properties," *IEEE Transactions on Antennas and Propagation*, Vol.: 47, No. 4, April 1999.

[20] S. Richter and R. de Carlo, "Continuation methods: theory and applications," *IEEE Transactions on Automatic Control*, Vol. 28, pp. 660-665, 1983.

[21] *NIST Chemistry WebBook.* Available: http://webbook.nist.gov/chemistry/fluid/

TECHNICAL PUBLICATIONS

1. Sung Hyun Nam, Chun Zhan, Jon Lee, Corey Hahn, Karl Reichard*, Paul Ruffin+, Kung-Li Deng++, and Shizhuo Yin, "Bend-insensitive ultra short long-period gratings by the electric arc method and their applications to harsh environment sensing and communication," Optics Express Vol. 13, pp. 731-737 (2005).

2 S. Nam and S. Yin, "High temperature sensing using Whispering Gallery Mode Resonance in bent optical fibers," IEEE Photonic Technology Letters, pp. 2391-2393 (2005).

3. Wei-Hung Su*, Kebin Shi, Zhiwen Liu, Bo Wang, Karl Reichard+, and Shizhuo Yin, " A large-depth-of-field projected fringe profilometry using supercontinuum light illumination," Optics Express Vol. 13, pp. 1025-1032 (2005).

4. Yi Yang, Jon Lee, Karl Reichard*, Paul Ruffin+, Frank Liang,++, Dave Ditto+++, and Shizhuo Yin, "Fabrication and implementation of a multi-to-single mode converter based on a tapered multimode fiber," Optics Communications, pp. 129-137 (2005).

5. Kun-Wook Chung and Shizhuo Yin, "Design of a tunable phase-shifted long period grating using partial etching technique," Microwave and Optics Technology Letters, pp. 18-21 (2005).

6. B. Wang, J. Fu, Y. Liu, R. Guo, and S. Yin, "Vector sensing with electronic fiber speckle pattern interferometry," SPIE 5911, pp.59110O-1 – 59110O-10, San Diego, CA, August 1, 2005.

7. S. Yin, K. Deng, S. Nam, and K. Reichard, "Fiber optic high temperature sensing based on whispering gallery mode resonance," SPIE 5911, pp. 59110W-1 – 59110W-10, San Diego, CA, August 1, 2005.

8. F. Wu, Y. Yang, and S. Yin, "High precision fiber taper fabrication using the self-immersion depth control in chemical etching," SPIE 5911, pp.59110x-1 – 59110x-10, San Diego, CA, August 1, 2005.

9. Sung-Hyun Nam, Jon Lee, Shizhuo Yin, Karl Reichard, Paul Ruffin, and Qing Wang, "Ultrasensitive fiber optic sensors and their applications," SPIE 5691 pp. 120-128, San Jose, CA, 2005

10. Stuart (Shizhuo) Yin, Sung-Hyun Nam, Yi Yang, Chun Zhan, and Kun-Wook Chung, "Innovative Fiber Optic Gratings: Fabrications and Applications," Proceedings of International Symposium on Advances and Trends in Fiber Optics and Applications, October 11-15, 2004, Chongqing University, Chongqing, China.

11. B. H. Kim, J. P. Velas, and K. Y. Lee, "Semigroup based neural network architecture for extrapolation of enthalpy in a power plant," *Proceedings of the ISAP*, pp. 291-296, 2005.

12. K. Y. Lee, J. P. Velas, and B. H. Kim, "Development of an intelligent monitoring system with high temperature distributed fiberoptic sensor for fossil-fuel power plants," *IEEE Power Engineering Society General Meeting*, pp. 1350-1355, Jun 6-10, 2004.

ON-SITE VISIT

We had an on-site visit from DOE on March 23, Wednesday, 2005. The following is the itinerary:

I. 8:30 am - 8:40 opening remarks
DOE: Susan Maley, Robert Romanosky, Peter Muchunas
PSU: Kwang Lee, Stuart Yin, Andre Boehman, and Graduate Students (Mel Fox, Byong-Hee Kim)
The Energy Institute, 405 Academic Activities Building

2. 8:40 - 9:30 am presentation

3. 9:30 - 10:00 lab tour at Energy Institute

4. 10:00 - 11:00 am travel to EE building and Lab tour at EE

Dr. Lee's Intelligent Distributed Controls Research Lab, 104 EE East
Dr. Yin's optics lab - In particular, harsh environment fiber optic grating fabrication facilities, EE East

5. 11:00 - 11:30 am, 129 EE East
Closing remarks.

REVIEW MEETING

We attended the annual review meeting held in June 2005 in Pittsburgh, PA.